

Ultra-fast magnetisation rates within the Landau-Lifshitz-Bloch model.

U. Atxitia and O. Chubykalo-Fesenko

Instituto de Ciencia de Materiales de Madrid, CSIC, Cantoblanco, 28049 Madrid, Spain

The ultra-fast magnetisation relaxation rates during the laser-induced magnetisation process are analyzed in terms of the Landau-Lifshitz-Bloch (LLB) equation for different values of spin S . The LLB equation is equivalent in the limit $S \rightarrow \infty$ to the atomistic Landau-Lifshitz-Gilbert (LLG) Langevin dynamics and for $S = 1/2$ to the M3TM model [B. Koopmans, *et al.* Nature Mat. **9** (2010) 259]. Within the LLB model the ultra-fast demagnetisation time (τ_M) and the transverse damping (α_{\perp}) are parameterized by the intrinsic coupling-to-the-bath parameter λ , defined by microscopic spin-flip rate. We show that for the phonon-mediated Elliott-Yafet mechanism, λ is proportional to the ratio between the non-equilibrium phonon and electron temperatures. We investigate the influence of the finite spin number and the scattering rate parameter λ on the magnetisation relaxation rates. The relation between the fs demagnetisation rate and the LLG damping, provided by the LLB theory, is checked basing on the available experimental data. A good agreement is obtained for Ni, Co and Gd favoring the idea that the same intrinsic scattering process is acting on the femtosecond and nanosecond timescale.

PACS numbers: 75.40.Gb, 78.47.+p, 75.70.-i

I. INTRODUCTION

Magnetisation precession and the spin-phonon relaxation rates at picosecond timescale were considered to be the limiting factor for the speed of the magnetisation switching^{1,2}, until using optical excitation with fs pulsed lasers the possibility to influence the magnetisation on femtosecond timescale was demonstrated³⁻⁶. The ultra-fast laser-induced demagnetisation immediately became a hot topic of solid state physics due to an appealing possibility to push further the limits of operation of magnetic devices. This ultra-fast process has now been shown to proceed with several important characteristic timescales⁶: (i) the femtosecond demagnetisation with timescale τ_M (ii) the picosecond recovery with timescale τ_E and (iii) the hundred picoseconds -nanosecond magnetisation precession, traditionally characterized by the ferromagnetic resonance frequency ω_{FMR} and the Landau-Lifshitz-Gilbert damping parameter α_{LLG} (see Fig.1).

The physics of the magnetisation changes on femto-second timescales is obviously not-trivial and will require novel theories within the relativistic quantum electrodynamics of many electron systems. From theoretical point of view, the existing models try to answer an open question of the role of different subsystems (photons, phonons, electrons and spins) in the ultra-fast angular momentum transfer⁷. This common goal is stimulated by experimental findings provided by the XMCD measurements showing the important role of the spin-orbit interactions^{8,9}. For the present state of art quantum mechanical descriptions^{8,10-13} of ultra-fast demagnetisation processes involve unavoidable simplifications and sometimes even some ad-hoc assumptions necessary to explain experimental findings, such as reduced exchange interactions, enhanced spin-orbit coupling or a Gaussian distribution of occupied states around the Fermi level. While some degree of agreement has been achieved in modelling of the ultra-fast demagnetisation (τ_M) scale¹⁴, the modelling of all three ultra-fast demagnetisation rates within the same approach is outside the possibilities of the quantum mechanical approaches.

The three-temperature (3T) phenomenological model in-

volves the rate equations for the electron, phonon and spin temperatures (energies)^{10,15-17}. Recently, it has been shown that the introduction of the spin temperature is not adequate¹⁸ since the spin system is not in the equilibrium on the femtosecond timescale. It has been suggested to couple the spin dynamics to the two-temperature (2T) model for phonon and electron temperatures¹⁸⁻²². These models are based on the energy flow picture and leave unidentified the angular momentum transfer mechanism and the underlying quantum mechanism responsible for the spin flip²². They essentially interpret the ultra-fast demagnetisation as "thermal" processes, understanding the temperature as energy input from photon to electron and then to the spin system. By using these models the important role of the linear reversal path in the femtosecond demagnetisation has been identified^{23,24}. The comparison with experiment seems to indicate that in order to have magnetisation switching in the ultra-fast timescale, a combined action of "heat" and large field coming from the inverse Faraday effect is necessary²⁴.

The most successful recent phenomenological models describing the ultra-fast magnetisation dynamics are (i) the Langevin dynamics based on the Landau-Lifshitz-Gilbert (LLG) equation and classical Heisenberg Hamiltonian for localized atomic spin moments^{18,19}, (ii) the Landau-Lifshitz-Bloch (LLB) micromagnetics^{21,22} and (iii) the Koopmans's magnetisation dynamics model (M3TM)²⁵. The spin dynamics could be coupled to the electron temperature from the 2T model, underlying the electronic origin of the spin-flip process^{18,19,21,22,24} or to both electron and phonon temperatures, underlying the Elliott-Yafet mechanism mediated by phonons²⁵. When the 2T model was carefully parameterised from the measured reflectivity, it gave an excellent agreement with the experiment in Ni²² using the former approach or in Ni, Co and Gd using the latter approach²⁵.

In the classical derivation of the LLB equation the thermal averaging has been performed analytically within the mean field (MFA) approximation²⁶. Thus, the LLB equation for classical spins ($S \rightarrow \infty$) is equivalent to an ensemble of exchange-coupled atomistic spins modelled by stochas-

tic LLG equations^{20,27}. At the same time, in some cases the LLB equation may be preferable with respect to the atomistic Heisenberg model, since being micromagnetic it can incorporate quantum nature of magnetism and the quantum derivation of LLB also exists²⁸. In particular the limits of validity for the statistical mechanics based on the classical Heisenberg model for the description of materials with delocalized magnetism of d -electrons in transition metals or magnetism of f -electrons in rare earths are not clear. An alternative statistical simplified description of d -metals consists of a two level system with spin-up and spin-down bands (i.e. $S = \pm 1/2$), as has been done by B. Koopmans *et al.*²⁵. Their model, as we show in the present article, is also equivalent to the quantum LLB equation with spin $S = 1/2$. An additional advantage in the use of the LLB equation is the possibility to model larger spatial scales^{20,21}. Therefore the LLB micromagnetics is an important paradigm within the multiscale magnetisation dynamics description. The LLB equation has been shown to describe correctly the three stages of the ultra-fast demagnetisation processes: the sub-picosecond demagnetisation, the picosecond magnetisation recovery and the nanosecond magnetisation precession²⁰⁻²², see Fig.1.

The intrinsic quantum mechanical mechanisms responsible for the ultra-fast demagnetisation in the LLB model are included in the intrinsic coupling-to-the-bath parameter λ ^{22,28}. The coupling process is defined by the rate of the spin flip. Several possible underlying quantum mechanisms are currently under debate: the Elliott-Yafet (EY) electron scattering mediated by phonons or impurities^{13,25}, or other electrons¹⁴ and electron-electron inelastic exchange scattering^{29,30}. By combining the macroscopic demagnetisation equation (M3TM model) with the rate of spin flip calculated on the basis of full Hamiltonian, Koopmans *et al.*²⁵ have been able to relate the ultra-fast demagnetisation time τ_M with the spin flip rate of the phonon-mediated Elliott-Yafet scattering. The authors fitted experimental demagnetisation rates in Ni, Co, Gd to the phenomenological M3TM model and found them to be consistent with the values estimated on the basis of ab-initio theory¹³. The coupling-to-the-bath parameter λ (microscopic damping parameter in atomistic LLG model) should be distinguished from that of the macroscopic damping α_{LLG} (α_{\perp} in the LLB model), a more complicated quantity which includes the magnon-magnon processes.

The first attempt to relate the sub-picosecond demagnetisation time with the macroscopic damping processes was given by Koopmans *et al.*⁶ who suggested the relation $\tau_M \sim 1/\alpha_{LLG}$. Subsequently and with the aim to check this relation several experiments in doped permalloy were performed³²⁻³⁴. The permalloy thin films were doped with rare earth impurities, allowing to increase in a controlled way the damping parameter α_{LLG} . The effect on the demagnetisation time τ_M was shown to be opposite³⁴ or null³², in contrast to the above relation. However, it should be noted that the analysis leading to this expression was performed in terms of the Landau-Lifshitz-Gilbert equation, relating the ultra-fast demagnetisation time τ_M to the transverse damping without taking into account their temperature dependence. Moreover, one should take into account that the rare-earth impurities may introduce a different

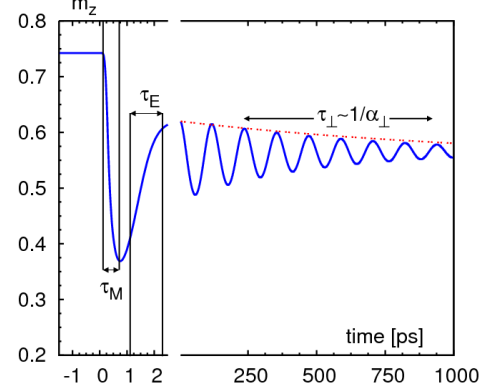


Figure 1. Characteristic time scales in ultrafast laser-induced magnetisation dynamics experiments. The curve is obtained by the integration of the Landau-Lifshitz-Bloch equation coupled to the two-temperature model with the parameters from Ref.21. For the modelling of precession the applied field $H_{ap} = 1\text{ T}$ at 30 degrees was used.

scattering mechanism with a slower timescale³³.

Partially basing on the above mentioned experimental results and from a general point of view, the longitudinal relaxation (the ultra-fast demagnetisation rate τ_M) and the transverse relaxation (the LLG damping α_{LLG}) may be thought to be independent quantities. Indeed, different intrinsic and extrinsic mechanisms can contribute to the demagnetisation rates at different timescales. One can, for example, mention that during the femtosecond demagnetisation the electron temperature is often raised up to the Curie temperature^{22,24}. At this moment, the high frequency THz spinwaves^{35,36} including the Stoner excitations³⁰ contribute. At the same time, the transverse relaxation is related to the homogeneous precessional mode. The LLB equation takes care of the different natures of longitudinal and transverse relaxation, arising from the spin disordering. The LLB model calculates them independently but basing on the same intrinsic scattering mechanism parameterized by the parameter λ . The increment of the number of scattering events is mimicked by the increases of the electron temperature. Consequently, the relation between the ultra-fast demagnetisation and precession remains valid but with a temperature-dependent correction. If this relation is confirmed experimentally, a unique intrinsic coupling parameter means that the same main microscopic mechanism is acting on both timescales. In the present article we will show that the analysis of the available experimental data seems to indicate towards this possibility, at least in pure transition metals such as Ni or Co and in rare earth metal Gd. We did not find validity of the corresponding relation in Fe.

Up to now only classical version ($S \rightarrow \infty$) of the LLB equation was used to model the ultra-fast demagnetisation processes^{20,21,24}. In the present article we show the important role of the choice of the quantum spin value, resulting in the differences in the corresponding longitudinal relaxation times. The article is organized as follows. In section II we present different formulations of the quantum LLB model and its main features for different spin values S . In section III

we present results on the modelling of the demagnetisation processes within LLB models with different choices of the quantum spins number S and of the intrinsic scattering mechanisms. In section IV we present our attempts to link the ultra-fast demagnetisation rates in transition metals and Gd and comparison with available experimental data. Section V concludes the article. In the Appendix to the article we demonstrate the equivalence of the LLB model with $S = 1/2$ and the M3TM model by B. Koopmans *et al.*²⁵.

II. THE LANDAU-LIFSHITZ-BLOCH MODEL WITH QUANTUM SPIN NUMBER S .

The LLB equation for a quantum spin was derived from the density matrix approach²⁸. Although the model Hamiltonian was rather the simplest form of the spin-phonon interaction, the generalization of the approach should be possible to more complex situations. The macroscopic equation for the magnetisation dynamics, valid at all temperatures, is written in the following form:

$$\dot{\mathbf{n}} = \gamma[\mathbf{n} \times \mathbf{H}] + \frac{\gamma\alpha_{\parallel}}{n^2} [\mathbf{n} \cdot \mathbf{H}_{\text{eff}}] \mathbf{n} - \frac{\gamma\alpha_{\perp}}{n^2} [\mathbf{n} \times [\mathbf{n} \times \mathbf{H}_{\text{eff}}]] \quad (1)$$

where $n = M/M_e(T) = m/m_e$ is the reduced magnetisation, normalized to the equilibrium value M_e at given temperature T and $m = M/M_e(T = 0K)$. The effective field \mathbf{H}_{eff} , contains all usual micromagnetic contributions, denoted by \mathbf{H}_{int} (Zeeman, anisotropy, exchange and magnetostatic) and is augmented by the contribution coming from the temperature

$$\mathbf{H}_{\text{eff}} = \mathbf{H}_{\text{int}} + \frac{m_e}{2\tilde{\chi}_{\parallel}} (1 - n^2) \mathbf{n}, \quad (2)$$

where $\tilde{\chi}_{\parallel}(T) = (\partial m / \partial H)_{H \rightarrow 0}$ is the longitudinal susceptibility. The LLB equation contains two relaxational parameters: transverse α_{\perp} and longitudinal α_{\parallel} , related to the intrinsic coupling-to-the-bath parameter λ . In the quantum description the coupling parameter λ contains the matrix elements representing the scattering events and, thus, is proportional to the spin-flip rate due to the interaction with the environment. This parameter, in turn, could be temperature dependent and, in our opinion, it is this microscopic parameter which should be related to the Gilbert parameter calculated through ab-initio calculations as in Refs.^{38,39}, since the contribution coming from the spin disordering is not properly taken into account in these models. In the quantum case the temperature dependence of the LLB damping parameters is given by the following expressions:

$$\alpha_{\parallel} = \frac{\lambda}{m_e} \frac{2T}{3T_C} \frac{2q_S}{\sinh(2q_S)} \xrightarrow{S \rightarrow \infty} \frac{\lambda}{m_e} \frac{2T}{3T_C}, \quad (3)$$

$$\alpha_{\perp} = \frac{\lambda}{m_e} \left[\frac{\tanh(q_S)}{q_S} - \frac{T}{3T_C} \right] \xrightarrow{S \rightarrow \infty} \frac{\lambda}{m_e} \left[1 - \frac{T}{3T_C} \right], \quad (4)$$

with $q_S = 3T_C m_e / [2(S+1)T]$, where S is the quantum spin number and T_C is the Curie temperature. In the case $S \rightarrow \infty$ the damping coefficients have the forms used in several previously published works⁴⁰, suitable for the comparison with the Langevin dynamics simulations based on the classical Heisenberg Hamiltonian and in agreement with them^{20,27}.

Eq.(1) is singular for $T > T_C$, in this case it is more convenient to use the LLB equation in terms of the variable $m = M/M_e(T = 0K)$ ²⁷. The corresponding LLB equation is indistinguishable from Eq.(1) but with different relaxational parameters $\tilde{\alpha}_{\parallel} = m_e \alpha_{\parallel}$, $\tilde{\alpha}_{\perp} = m_e \alpha_{\perp}$ and $\tilde{\alpha}_{\perp} = \tilde{\alpha}_{\parallel}$ for $T > T_C$, in this case the contribution of temperature to \mathbf{H}_{eff} [the second term in Eq.(2)] is $(-1/\tilde{\chi}_{\parallel})[1 - 3T_C m^2 / 5(T - T_C)m] \mathbf{m}$. Although this formulation is more suitable for the modelling of the laser-induced demagnetisation process, during which the electronic temperature is usually raised higher than T_C , it is the expression (4) which should be compared with the transverse relaxation parameter α_{LLG} due to the similarity of the formulation of the Eq.(1) with the macromagnetic LLG equation. In the classical case and far from the Curie temperature $T \ll T_C$, $\lambda = \alpha_{\perp} = \tilde{\alpha}_{\perp}$ (α_{LLG}).

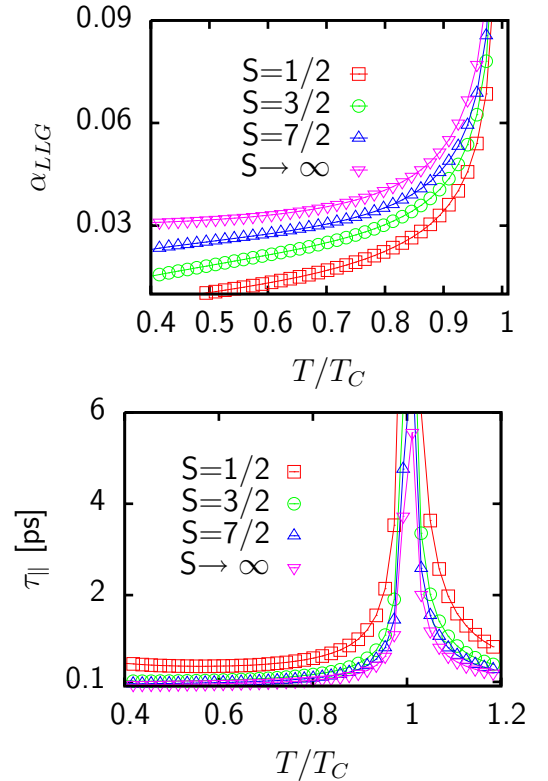


Figure 2. (Up) The transverse damping parameter α_{\perp} (α_{LLG}) as a function of temperature within the LLB model for different spin values S . The intrinsic coupling parameter was set to $\lambda = 0.03$. (Down) The longitudinal relaxation time τ_{\parallel} as a function of temperature within the LLB model for different spin values S . The temperature-dependent magnetisation and the longitudinal susceptibility $\tilde{\chi}_{\parallel}$ were evaluated in both cases in the MFA approach using the Brillouin function.

In the "thermal" model the nature of the longitudinal and

the transverse relaxation differs from the point of view of characteristic spinwave frequencies. The transverse relaxation (known as the LLG damping) is basically the relaxation of the FMR mode. The contribution of other spinwave modes is reduced to the thermal averaging of the micromagnetic parameters and the main effect comes from the decrease of the magnetisation at high temperature. Consequently, the transverse damping parameter increases with temperature (see Fig.2), consistent with atomistic modelling results²⁷ and well-known FMR experiments^{37,41}.

On the contrary, the main contribution to the longitudinal relaxation comes from the high-frequency spin waves. This process occurs in a strong exchange field. As a result, the longitudinal relaxation time (the inverse longitudinal relaxation) is much faster and increases with temperature, known as critical slowing down, see Fig.2. This slowing down has been shown to be responsible for the slowing down of the femto-second demagnetisation time τ_M as a function of laser pump fluency^{18,22}. The characteristic longitudinal timescale is not only defined by the longitudinal damping parameter (3) but also by the temperature-dependent longitudinal susceptibility $\tilde{\chi}_{\parallel}(T)$ ²⁷, according to the following equation:

$$\tau_{\parallel}(T) = \frac{\tilde{\chi}_{\parallel}(T)}{\gamma\tilde{\alpha}_{\parallel}(T)}. \quad (5)$$

As it can be observed in Fig. 2 the transverse relaxation parameter α_{\perp} (α_{LLG}) and the longitudinal relaxation time τ_{\parallel} have a strong dependence on the quantum spin number S chosen to describe system's statistics. We conclude here about the occurrence of quite different relaxation rates for the two extreme cases $S = 1/2$ and $S = \infty$.

B. Koopmans *et al.* recently used a different equation to describe the ultrafast demagnetisation dynamics²⁵, called M3TM model:

$$\frac{dm}{dt} = Rm \frac{T_p}{T_C} \left(1 - m \coth \left(\frac{mT_C}{T_e} \right) \right). \quad (6)$$

Eq.(6) has been obtained through the general Master equation approach for the dynamics of the populations of a two level system (spin $S = 1/2$ was used) with the switching probability evaluated quantum-mechanically for the phonon-mediated EY spin-flips. Here T_p and T_e are phonon and electron temperatures, respectively, and R is a material specific parameter, related to the spin-flip probability in the phonon-mediated EY scattering events a_{sf} , as

$$R = \frac{8a_{sf}G_{ep}\mu_B k_B V_a T_C^2}{\mu_{at} E_D^2}, \quad (7)$$

where V_a and μ_{at} are the atomic volume and magnetic moment, respectively, G_{ep} is the electron-phonon coupling constant, k_B is the Boltzmann constant, μ_B is the Bohr magneton and E_D is the Debye energy. This equation has allowed to fit the ultrafast demagnetisation time (τ_M) obtaining the values of R in Ni, Co and Gd²⁵ and relating them to the phonon-mediated EY scattering rates a_{sf} .

As we show in the Appendix, the M3TM equation (6) corresponds to the longitudinal part of the LLB equation with

thermal field only ($\mathbf{H}_{int} = 0$) and with spin $S = 1/2$, i.e. it is equivalent to

$$\frac{dm}{dt} = \gamma\tilde{\alpha}_{\parallel} H_{eff}. \quad (8)$$

This gives a relation between the intrinsic coupling parameter λ and the material specific parameter R and finally with the phonon-mediated EY spin-flip probability a_{sf} via the formula:

$$\lambda = \frac{3R}{2\gamma} \frac{\mu_{at}}{k_B T_C} \frac{T_p}{T_e} = \lambda_0 \frac{T_p}{T_e}. \quad (9)$$

Thus the two approaches are reconciled, provided that the temperature-dependent coupling rate (9) is used in the LLB equation, in contrast to other works^{18,21,22} where the coupling λ is considered to be temperature-independent. Combining expressions (5) (7) and (9), one can immediately see that in the case of the phonon-mediated EY process, the longitudinal relaxation time is determined by

$$\tau_{\parallel} \propto \frac{\tilde{\chi}_{\parallel}}{a_{sf}} \frac{E_D^2}{G_{ep} V_a T_p}. \quad (10)$$

In Ref.25 and basing on the phonon-mediated EY picture, the classification of materials on the basis of the "magnetic interaction strength" parameter μ_{at}/J was proposed, where J is the material exchange parameter. According to the expression above, the demagnetisation rate depends on more parameters, among which the important one is also the electron-phonon coupling G_{ep} defining how fast the electron system can pass the energy to the phonon one. Another important parameter is the microscopic spin-flip rate a_{sf} . Comparing to the B. Koopmans *et al.*²⁵ materials classification, the longitudinal susceptibility in Eq.(10) is indeed defined by the value of the atomic moment μ_{at} and by the fact that this function rapidly increases with temperature and diverges close to $T_C \propto J$. At $T \approx T_C$ one obtains a simple linear relation²⁷ $\tilde{\chi}_{\parallel} \propto \mu_{at}/J$, thus showing the dependence of the demagnetisation rate on this parameter, as suggested in Ref.25.

In the case of the phonon-mediated EY process the temperature dependence of the longitudinal relaxation is coming from the longitudinal susceptibility only (cf. Eq. (10)), as opposed to the case $\lambda = \text{const}$ (cf. Eq.(5)). (We do not discuss here the possibility that the phonon-mediated EY spin-flip rate a_{sf} may be also temperature dependent.) However, the temperature dependence of the susceptibility is characterized by its exponential divergence close to T_C . In these circumstances an additional linear temperature dependence provided by the longitudinal damping is difficult to distinguish in the fitting procedure of experimental data.

III. MODELLING OF THE LASER-INDUCED ULTRA-FAST DEMAGNETISATION WITHIN THE LLB MODELS.

In the spirit of Refs.^{18,20–22,25} for the modelling of ultra-fast demagnetisation dynamics, the LLB equation may be coupled

to the electron temperature T_e only, understanding the electrons as the main source for the spin-flip mechanism^{18,20–22} or to both phonon and electron temperatures in the spirit of the phonon-mediated Elliott-Yafet process²⁵. In both cases it is the electron temperature $T = T_e$ which couples to the magnetisation in the LLB formalism, since the phonon temperature could only enter into the temperature dependence of the coupling-to-the bath parameter λ via Eq.(9). Note that the temperature T is not the spin temperature, since the resulting dynamics is taking place out-of-equilibrium.

The electron T_e and phonon T_p temperatures are taken from the two-temperature (2T) model^{15,45,46}. Within this model their dynamics is described by two differential equations:

$$\begin{aligned} C_e \frac{dT_e}{dt} &= -G_{ep}(T_e - T_p) + P(t), \\ C_p \frac{dT_p}{dt} &= G_{ep}(T_e - T_p). \end{aligned} \quad (11)$$

Here $C_e = \gamma_e T_e$ ($\gamma_e = \text{const}$) and C_p are the specific heats of the electrons and the lattice. The Gaussian source term $P(t)$ is a function which describes the laser power density absorbed in the material. The function $P(t)$ is assumed to be proportional to the laser fluence F with the proportionality coefficient which could be obtained from the long time scale demagnetization data (for which $T_e = T_p$)²². The dynamics of the electron temperature can be also measured directly in the time-resolved photoemission experiment⁴⁷.

The first of Eqs.(11) may also include a diffusion term $\nabla_z(\kappa \nabla_z T_e)$ taking into account a final penetration depth of the deposited energy into the film thickness²⁵ and a term, $C_e(T_e - 300\text{K})/\tau_{th}$ describing the heat diffusion to the external space²². In the present article, the parameters for the 2T-model were taken either from Koopmans *et al.*²⁵ or from U. Atxitia *et al.*²² (for Ni only), where they were carefully parameterized through the reflectivity measurements. The Ni (Co, Gd etc) parameters, such as magnetisation as a function of temperature were taken assuming the Brillouin (Langevin for $S \rightarrow \infty$) function.

The coupling of the 2T model to the LLB equation adequately describes all three stages of the ultra-fast demagnetisation rates: sub-ps demagnetisation, ps recovery and sub-ns precession^{21,22}, see Fig.1. As a consequence of the temperature dependence of both longitudinal damping and susceptibility, and since the temperature is dynamically changed according to Eqs.(11), the longitudinal relaxation time is time-dependent via Eq.(5). It is also strongly dependent on the parameters of the 2T model and its dynamics is not simple. Consequently, the sub-ps ultra-fast demagnetisation generally speaking is not exponential and cannot be described in terms of one relaxation time τ_M . Simple analytical expression is possible to obtain with the supposition of a square-shaped temperature pulse²³. The two-exponential fitting is also often used^{22,36}. In our approach the fs demagnetisation is fitted directly to the solution of the LLB equation without assumption of the one- or two-exponential decay. However, to comply with the existing approaches, we still discuss the demagnetisation rate in terms of a unique parameter τ_M .

In the experiment performed in the same material the only

remaining fitting parameter for the LLB model is the coupling parameter λ . The choice of λ together with the parameters of the 2T model defines all magnetisation rates. In Fig.3 we present modelling of the ultra-fast demagnetisation and remagnetisation for various values of the coupling parameter λ , chosen to be independent on temperature, as in Ref. 22. If for some reason the scattering channel was suppressed, this would lead to a small scattering rate and consequently a small demagnetisation and a slow recovery. Indeed, the value of λ for Gd was found to be 60 times smaller than for Ni (see Table I). This small value of λ assures a large delay in the magnetisation relaxation towards the equilibrium electron temperature. Thus this parameter defines the diversity of the demagnetisation rates in larger extent than the ratio μ_{at}/J , suggested in Ref.25 and discussed in the previous subsection.

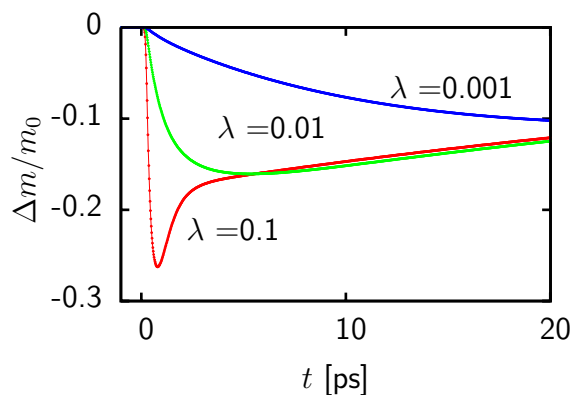


Figure 3. The result of integration of the LLB model ($S \rightarrow \infty$) with different parameters λ (increasing from top to the bottom). In this case the the 2T model parameters were taken from Ref.22 with laser fluence $F = 30 \text{ mJ/cm}^2$

Another parameter strongly influencing the demagnetisation rates is the phonon-electron coupling G_{ep} defining the rate of the electron temperature equilibration time. This is the main parameter governing the magnetisation recovering time τ_E . Indeed, in Ref.²⁵ the phonon-electron coupling G_{ep} was chosen to be 20 times smaller for Gd than for Ni. By adjusting this parameter, the ultra-slow demagnetisation rates observed in TbFe alloy⁴⁸, Gd⁴⁹ and in half-metals⁵⁰ as well as the two time-scales demagnetisation^{25,49} are also well-reproduced (see, as an example, Fig.4). Within this model the two-time scale process consists of a relatively fast demagnetisation (however much slower than in Ni), defined by the electron temperature and small value of λ , followed by a much slower process due to a slow energy transfer from the electron to the lattice system.

As it was mentioned in the previous subsection, the phonon-mediated EY mechanism predicts the coupling to the bath parameter λ to be dependent on the ratio between the phonon and electron temperature through the relation (9). A decrease of λ up to two times at high fluencies is observed for Ni and Co. The analysis of the data presented in Ref. 25 and 47 for Gd has shown that during the demagnetisation process the ratio T_e/T_p has increased almost 6 times. In Fig.5 we present the magnetisation dynamics for Ni evaluated for

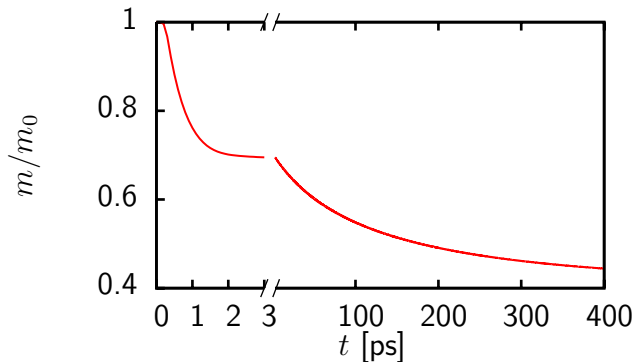


Figure 4. The result of integration of the LLB model ($S \rightarrow \infty$) with constant $\lambda_0 = 0.0015$ (see Table I). In this case the 2T model parameters were taken from Ref.25 corresponding to Gd.

two laser pulse fluencies, assuming various values of the spin S and temperature-dependent and independent λ values. Note quite different demagnetisation rates at high fluency for two limiting cases $S = 1/2$, used in Ref.25 and $S = \infty$, used in Ref.22. The differences in the choice of λ are pronounced at high pump fluency but are not seen at low fluency. One can also hope that in the fitting procedure of experimental data it would be possible to distinguish the two situations. Unfortunately, the fitting to experimental data procedure is complicated and the changes coming from the two cases described above are competing with several different possibilities such as an additional temperature dependency in electron or phonon specific heats⁵¹. Additionally, we would like to mention different electron-phonon coupling constants G_{ep} used in Refs. 22 and 25. Fitting to experimental data from Ref.25 for Ni for high fluency, we have found that the case of the temperature-dependent $\lambda = \lambda_0(T_p/T_e)$ can be equally fitted with the temperature-independent $\lambda \approx \lambda_0/2$. To answer definitely which fitting is better, more experimental data promoting one or another intrinsic mechanism and varying laser fluency is necessary.

IV. LINKING DIFFERENT TIMESCALES

Since the longitudinal relaxation occurs under strong exchange field and the transverse relaxation - under external applied field, their characteristic timescales are quite different. However, the LLB equation provides a relation between the ultra-fast demagnetisation (longitudinal relaxation) and the transverse relaxation (ordinary LLG damping parameter) via the parameter λ_0 ($\lambda = \lambda_0$ or $\lambda = \lambda_0(T_p/T_e)$ for $T_p = T_e$). The two demagnetisation rates could be measured independently by means of the ultra-fast laser pump-probe technique⁵². It has been recently demonstrated⁵³ that the damping of the laser-induced precession coincides with the measured by FMR in transition metals. By separate measurements of the two magnetisation rates, the relations (4) and (5) given by the LLB theory could be checked. This can provide the validation of the LLB model, as well as the answer to the question if the same microscopic mechanism is acting on

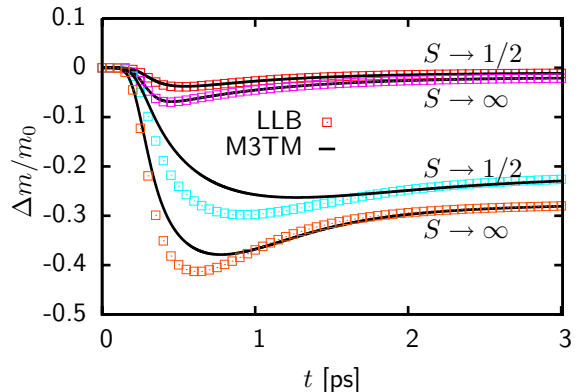


Figure 5. Magnetisation dynamics during laser-induced demagnetisation process calculated within the LLB model with different spin numbers and for two laser-fluencies $F = 10 \text{ mJ/cm}^2$ (upper curves) and $F = 40 \text{ mJ/cm}^2$ (bottom curves). Ni parameters from Ref.22 were used. The symbols are calculated with the LLB equation with the intrinsic damping parameter using a constant $\lambda_0 = 0.003$ value, and the solid lines with the LLB equation and the intrinsic coupling with the temperature dependent $\lambda = \lambda_0(T_p/T_e)$.

femtosecond and picosecond timescales. Unfortunately, the damping problem in ferromagnetic materials is very complicated and the literature reveals the diversity of measured values in the same material, depending on the preparation conditions.

Thus, to have a definite answer the measurement on the same sample is highly desired. The measurements of both α_{\perp} and τ_M are available for Ni²² where an excellent agreement between ultra-fast magnetisation rates via a unique temperature-independent parameter $\lambda = 0.04$ has been reported²². The results of the systematic measurements of τ_M are also available for Ni, Co, Gd in Ref. 25, as well as for Fe⁵⁵. The next problem which we encounter here is that the demagnetisation rates strongly depend on the spin value S , as is indicated in Figs. 2 and 5. The fitting of experimental data using LLB model with different S values results in different values of the coupling parameter λ_0 . The use of $S = 1/2$ value²⁵ or $S = \infty$ value²² is quite arbitrary and these values do not coincide with the atomic spin numbers of Ni, Co, Gd. Generally speaking, for metals the spin value is not a good quantum number. The measured temperature dependence of magnetisation, however, is well fitted by the Brillouin function with $S = 1/2$ for Ni and Co and $S = 7/2$ for Gd⁵⁴. These are the values of S which we use in Table I.

Consequently in Table I we present data for the coupling parameter λ_0 extracted from Ref.25. Differently to this article, for Gd we corrected the value of the parameter R to account for a different spin value by the ratio of the factors, i.e. $R^{S_1} = (f_{S_2}/f_{S_1})R^{S_2}$ with

$$f_S = \frac{2qs}{\sinh(2qs)} \frac{1}{m_{e,S}^2 \chi_{\parallel}^S}, \quad (12)$$

where the parameters are evaluated at 120K using the MFA expressions for each spin value S . The data are evaluated

Material	S	R^{25}	λ_0	α_{\perp}	α_{LLG}
Ni	1/2	17.2	0.0974	0.032	0.019 ⁴² -0.028 ⁴¹
Co	1/2	25.3	0.179	0.025	0.0036 ⁴¹ -0.006 ⁴³ -0.011 ⁴⁴
Gd	7/2	0.009	0.0015	0.00036	0.0005 ³³

Table I. The data for ultra-fast demagnetisation rate parameters for three different metals from ultrafast demagnetization rates and from FMR measurements. The third column presents the demagnetisation parameter R from Ref. 25, corrected in the case of Gd for spin $S = 7/2$. The fourth column presents the value of the λ_0 parameter, as estimated from the M3TM model²⁵ and the formula Eq.(9). The fifth column presents the data for α_{\perp} estimated via the LLB model Eq.(4) and the λ_0 value from the third column, at room temperature $T = 300K$ for Co and Ni and at $T = 120K$ for Gd. The last column presents the experimentally measured Gilbert damping collected from different references.

for the phonon-mediated EY process with the temperature-dependent parameter λ via the expression (9). The value of the Gilbert damping parameter α_{\perp} was then estimated through formula (4) at 300K (for Ni and Co) and at 120K for Gd. Note that for temperature-independent $\lambda = \lambda_0$ the resulting λ_0 and α_{\perp} values are approximately two times smaller for Ni and Co. The last column presents experimental values for the same parameter found in literature for comparison with the ones in the fifth column, estimated through measurements of the ultra-fast demagnetisation times τ_M and the relation provided by the LLB equation.

Given the complexity of the problem, the results presented in Table I demonstrate quite a satisfactory agreement between the values, extracted from the ultra-fast demagnetisation time τ_M and the Gilbert damping parameter α_{\perp} via one unique coupling-to-the-bath parameter λ . The agreement is particularly good for Ni, indicating that the same spin flip mechanism is acting on both timescales. This is true for both experiments in Refs.22 and 25. For Co the value is some larger. For the temperature-independent λ , the resulting value is two times smaller and the agreement is again satisfactory. We would like to note that no good agreement was obtained for Fe. The reported damping values⁴¹ are 5-10 times smaller as estimated from the demagnetisation rates measured in Ref. 55.

V. CONCLUSIONS

The Landau-Lifshitz-Bloch (LLB) equation provides a micromagnetic tool for the phenomenological modelling of the ultra-fast demagnetisation processes. Within this model one can describe the temperature-dependent magnetisation dynamics at arbitrary temperature, including close and above the Curie temperature. The micromagnetic formulation can take into account the quantum spin number. The LLB model includes the dynamics governed by both the atomistic LLG model and the M3TM model by Koopmans *et al.*²⁵. In the future it represents a real possibility for the multiscale modelling²⁰.

We have shown that within this model the ultra-fast demagnetisation rates could be parameterized through a unique

temperature dependent or independent parameter λ , defined by the intrinsic spin-flip rate. The magnetisation dynamics is coupled to the electron temperature through this parameter and is always delayed in time. The observed delay is higher for higher electron temperature. This is in agreement with the experimental observation that different materials demagnetize at different rates^{25,50} and that the process is slowed down with the increase of laser fluency. We have shown that for the phonon-mediated EY mechanism the intrinsic parameter λ is dependent on the ratio between phonon and electron temperatures and therefore is temperature dependent on the femto second - several picosecond timescale. The LLB equation can reproduce slow demagnetizing rates observed in several materials such as Gd, TbFe and half metals. This is in agreement with both phonon-mediated EY picture since in Gd a lower spin-flip probability was predicted and also with the inelastic electron scattering picture, since the electron diffusive processes are suppressed in insulators and half-metals^{31,50}. However, we also stress the importance of other parameters determining the ultra-fast demagnetisation rates, such as the electron-lattice coupling.

The macroscopic damping parameters (longitudinal and transverse) have different natures in terms of the involved spinwaves and in terms of the timescales. Their temperature dependence is different, however, they are related by the spin-flip rate. We have tried to check this relation in several transition metals such as Ni, Co, Fe and the rare-earth metal Gd. A good agreement is obtained in Co and Gd and an excellent agreement in Ni. This indicates that on both timescales the same main microscopic mechanism is acting. In Ni the agreement is good both within the assumptions $\lambda = \lambda_0$ and $\lambda = \lambda_0 T_p / T_e$. In Co the agreement seems to be better with the temperature-independent parameter $\lambda = \lambda_0$ which does not indicate towards the phonon-mediated EY mechanism. However, given a small discrepancy and the complexity of the damping problem, this conclusion cannot be considered definite. We can neither exclude an additional temperature dependence of the intrinsic scattering probability (i.e. the parameter λ_0) for both phonon-mediated EY and exchange scattering mechanisms which was not taken into account.

An open question is the problem of doped permalloy where an attempt to systematically change the damping parameter by doping with rare-earth impurities was undertaken³³ in order to clarify the relation between the LLG damping and the ultra-fast demagnetisation rate^{32,34}. The results are not in agreement with the LLB model. However in this case we think that the hypothesis of the slow relaxing impurities presented in Ref.34 might be a plausible explanation. Indeed, if the relaxation time of the rare earth impurities is high, the standard LLB model is not valid since it assumes an uncorrelated thermal bath. The correlation time could be introduced in the classical spin dynamics via the Landau-Lifshitz-Miyasaki-Seki approach⁵⁶. It has been shown that the correlation time of the order of 10 fs slows down the longitudinal relaxation independently on the transverse relaxation. Thus in this case, the modification of the original LLB model to account for the colored noise is necessary.

VI. ACKNOWLEDGEMENT

This work was supported by the Spanish projects MAT2007-66719-C03-01, CS2008-023.

Appendix A

To show the equivalence between the LLB model with $S = 1/2$ and the M3TM model²⁵, we compare the relaxation rates resulting from both equations. We start with the M3TM equation

$$\frac{dm}{dt} = -R \frac{T_p}{T_C} \left(1 - m \coth \left[\left(\frac{T_C}{T_e} \right) m \right] \right) m \quad (\text{A1})$$

where we identify the Brillouin function for the case $S = 1/2$, $B_{1/2} = \tanh(q)$ with $q = q_{1/2} = (T_C/T_e)m$. Now, we use the identity $B_{1/2} = 2/B'_{1/2} \sinh(2q)$ to write

$$\frac{dm}{dt} = -R \frac{T_p}{T_C} \left[\frac{2}{\sinh(2q)} \right] \left(1 - \frac{B_{1/2}}{m} \right) m^2 \quad (\text{A2})$$

we multiply and divide by $q\mu_{\text{at}}\beta$ to obtain

$$\frac{dm}{dt} = -R \frac{T_p}{T_C} \frac{\mu_{\text{at}}}{k_B T_C} \left[\frac{2q}{\sinh(2q)} \right] \left(\frac{1 - B_{1/2}}{m} \right) m \quad (\text{A3})$$

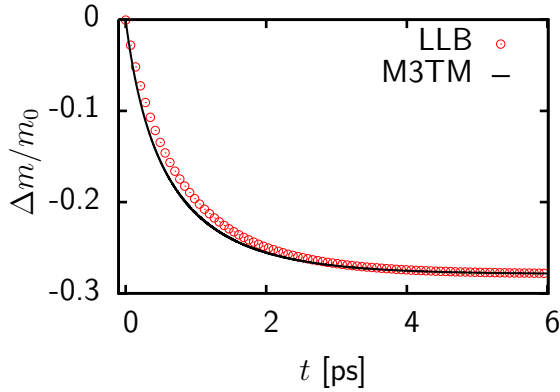


Figure 6. Longitudinal relaxation calculated with M3TM and LLB ($S=1/2$) models for Nickel parameters²² and $T/T_C = 0.8$.

We expand around equilibrium $m_e = B_{1/2}(q_e)$ the small quantity $1 - B_{1/2}/m$

$$1 - \frac{B_{1/2}(q)}{m} \cong \frac{\delta m}{m_e} \left(1 - \left(\frac{T_C}{T_e} \right) B'_{1/2}(q_e) \right) \quad (\text{A4})$$

where $\delta m = m - m_e$. Next, we expand m around m_e^2

$$m = m_e + \frac{1}{2} \frac{(m^2 - m_e^2)}{m_e} \implies \frac{\delta m}{m_e} = \frac{(m^2 - m_e^2)}{2m_e^2} \quad (\text{A5})$$

and,

$$\frac{1 - B_{1/2}/m}{\beta \mu_{\text{at}} B'_{1/2}} \approx \frac{1}{2\tilde{\chi}_{\parallel}} \frac{(m^2 - m_e^2)}{m_e^2} \quad (\text{A6})$$

Finally, collecting the equations (A3) and (A6) altogether:

$$\frac{dm}{dt} = \left(\frac{3R}{2} \frac{\mu_{\text{at}}}{k_B T_C} \right) \frac{2T_p}{3T_C} \frac{2q}{\sinh(2q)} \left(\frac{1}{2\tilde{\chi}_{\parallel}} \left(1 - \frac{m^2}{m_e^2} \right) m \right) \quad (\text{A7})$$

Comparing this to the LLB equation with longitudinal relaxation only and without anisotropy and external fields, we can write Eq. (A7) in terms of \mathbf{n} :

$$\frac{dn}{dt} = \gamma \frac{\lambda}{m_e} \frac{2T_e}{3T_C} \frac{2q}{\sinh(2q)} H_{\text{eff}} = \gamma \alpha_{\parallel} H_{\text{eff}} \quad (\text{A8})$$

where $H_{\text{eff}} = \frac{m_e}{2\tilde{\chi}_{\parallel}} (1 - n^2)n$, and

$$\alpha_{\parallel} = \left[\frac{3R}{2\gamma} \frac{\mu_{\text{at}}}{k_B T_C} \frac{T_p}{T_e} \right] \frac{2T_e}{3T_C} \frac{2q}{\sinh(2q)} \quad (\text{A9})$$

Thus the Koopmans' M3TM equation is equivalent to the LLB equation with $S = 1/2$ and where the precessional aspects are not considered. The link between both of them is the identification

$$\lambda = \frac{3R}{2\gamma} \frac{\mu_{\text{at}}}{k_B T_C} \frac{T_p}{T_e} \quad (\text{A10})$$

As an example we compare the result of the longitudinal relaxation in a numerical experiment for both M3TM and LLB ($S = 1/2$) equations. The system is put in a saturated state with $S_z/S = 1$ and we let it relax towards the equilibrium state. The comparison of the results for the temperature $T/T_C = 0.8$ are presented in Fig. 6.

¹ C. H. Back and D. Pescia, Nature **428**, 808 (2004).

² I. Tudosă, C. Stamm, A. B. Kashuba, F. King, H. C. Siegmann, J. Sthör, G. Ju, B. Lu and D. Weller, Nature **428**, 831 (2004).

³ E. Beaurepaire, J. C. Merle, A. Daunois and J.-Y. Bigot, Phys. Rev. Lett. **76**, 4250 (1996).

⁴ J. Hohlfeld, E. Matthias, R. Knorren and K. H. Bennemann, Phys. Rev. Lett. **78**, 4861 (1997).

⁵ A. Scholl, L. Baumgarten, R. Jacquemin and W. Eberhardt, Phys.

Rev. Lett. **79**, 5146 (1997).

⁶ B. Koopmans, M. van Kampen, J. T. Kohlhepp and W. J. M. de Jonge, Phys. Rev. Lett. **85**, 844 (2000).

⁷ C. Stamm, T. Kachel, N. Pontius, R. Mitzner, T. Quast, K. Holl-dack, S. Khan, C. Lupulescu, E. F. Aziz, M. Wiestruk, H. A. Dürr and W. Eberhardt, Nature Mat. **6**, 740 (2007).

⁸ J.-Y. Bigot, M. Vomir and E. Beaurepaire, Nature Phys. **5**, 515 (2009).

- ⁹ C. Boeglin, E. Beaurepaire, V. Halté, V. López-Flores, C. Stamm, N. Pontius, H. A. Dürr and J.-Y. Bigot, *Nature* **465**, 458 (2010).
- ¹⁰ G. Zhang, W. Hübner, E. Beaurepaire and J.-Y. Bigot in *Spin dynamics in confined magnetic structures I*, Topics Appl. Phys **83** 252 (2002), Springer-Verlag Berlin.
- ¹¹ G. P. Zhang, Y. Bai, W. Hübner, G. Lefkidis and T. George, *J. Appl. Phys.* **103**, 07B113 (2008).
- ¹² G. P. Zhang and W. Hübner, *Phys. Rev. Lett.* **85**, 3025 (2000).
- ¹³ D. Steiauf and M. Fähnle, *Phys. Rev. B* **79**, 140401 (R) (2009).
- ¹⁴ M. Krauß, T. Roth, S. Alebrand, D. Steil, M. Cinchetti, M. Aeschlimann and H. C. Schneider, *Phys. Rev. B* **80**, 180407(R) (2009).
- ¹⁵ M. I. Kaganov, I. M. Lifshitz and L. V. Tanatarov, *Sov. Phys. JETP* **4**, 173 (1957).
- ¹⁶ M. B. Agranat, S. I. Ashitkov, A. B. Granovski and G. I. Rukman, *Zh. Exp. Teor. Fiz.* **86**, 1376 (1984).
- ¹⁷ J. Hohlfeld, S.-S. Wellershoff, J. Güdde, U. Conrad, V. Jähnke and E. Matthias, *Chem. Phys.* **251**, 237 (2000).
- ¹⁸ N. Kazantseva, U. Nowak, R. W. Chantrell, J. Hohlfeld and A. Rebei, *Europhys. Lett.* **81**, 27004 (2008),
- ¹⁹ N. Kazantseva, D. Hinzke, U. Nowak, R. W. Chantrell and O. Chubykalo-Fesenko, *Phys. Stat. Sol.* **244**, 4389 (2007).
- ²⁰ N. Kazantseva, D. Hinzke, U. Nowak, R. W. Chantrell, U. Atxitia and O. Chubykalo-Fesenko, *Phys. Rev. B* **77**, 184428 (2008).
- ²¹ U. Atxitia, O. Chubykalo-Fesenko, N. Kazantseva, D. Hinzke, U. Nowak, R. W. Chantrell, *Appl. Phys. Lett.* **91**, 232507 (2007)
- ²² U. Atxitia, O. Chubykalo-Fesenko, J. Walowski, A. Mann and M. Münzenberg, *Phys. Rev. B* **81** 174401 (2010).
- ²³ N. Kazantseva, D. Hinzke, R. W. Chantrell and U. Nowak, *Europhys. Lett.* **86**, 27006 (2009)
- ²⁴ K. Vahaplar, A. M. Kalashnikova, A. V. Kimel, D. Hinzke, U. Nowak, R. Chantrell, A. Tsukamoto, A. Itoh, A. Kirilyuk and T. Rasing, *Phys. Rev. Lett.* **103**, 117201 (2009)
- ²⁵ B. Koopmans, G. Malinowski, F. Dalla Longa, D. Steiauf, M. Fähnle, T. Roth, M. Cinchetti and M. Aeschlimann, *Nature Mat.* **9**, 259 (2010).
- ²⁶ D. A. Garanin, *Phys. Rev. B* **55**, 3050 (1997)
- ²⁷ O. Chubykalo-Fesenko, U. Nowak, R. W. Chantrell and D. Garanin, *Phys. Rev. B* **74**, 094436 (2006).
- ²⁸ D. A. Garanin, *Physica A* **172**, 470 (1991).
- ²⁹ J. S. Hong and D. L. Mills, *Phys. Rev. B* **62** 5589 (2000).
- ³⁰ T. Balashov, A. F. Takacs, M. Dane, A. Ernst, P. Bruno, W. Wulfhekel, *Phys. Rev. B* **78**, 174404 (2008).
- ³¹ M. Battiato, K. Carva and P. M. Oppeneer, *Phys. Rev. Lett.* **105**, 027203 (2010).
- ³² J. Walowski, G. Müller, M. Djordjevic, M. Münzenberg, M. Kläui, C. A. F. Vaz, *Phys. Rev. Lett.* **101**, 237401 (2008).
- ³³ G. Woltersdorf, M. Kiessling, G. Meyer, J.-U. Thiele and C. H. Back, *Phys. Rev. Lett.* **102**, 257602 (2009).
- ³⁴ I. Radu, G. Woltersdorf, M. Kiessling, A. Melnikov, U. Bovensiepen, J.-U. Thiele and C. H. Back, *Phys. Rev. Lett.* **102**, 117201 (2009).
- ³⁵ E. Beaurepaire, G. M. Turner, S. M. Harrel, M. C. Beard, J.-Y. Bigot and C. A. Schmuttenmaer, *Appl. Phys. Lett.* **84**, 3465 (2004)
- ³⁶ M. Djordjevic and M. Münzenberg, *Phys. Rev. B* **75**, 012404 (2007)
- ³⁷ Y. Li, K. Baberschke and M. Farle, *J. Appl. Phys.* **69**, 4992 (1991).
- ³⁸ K. Gilmore, Y. U. Idzerda and M. D. Stiles, *Phys. Rev. Lett.* **99**, 027204 (2007).
- ³⁹ J. Kuneš and V. Kamberský, *Phys. Rev. B* **65**, 212411 (2002).
- ⁴⁰ D. A. Garanin and O. Chubykalo-Fesenko, *Phys. Rev. B* **70**, 212409 (2004)
- ⁴¹ S. M. Bhagat and P. Lubitz, *Phys. Rev. B* **10**, 179 (1974).
- ⁴² G. Dewar, B. Heinrich, and J. F. Cochran, *Can. J. Phys.*, **55**, 821 (1977)
- ⁴³ J. Lindner, I. Barsukov, C. Raeder, C. Hassel, O. Posth, R. Meckenstock, P. Landeros and D. L. Mills, *Phys. Rev. B* **88**, 224421 (2009).
- ⁴⁴ B. Heinrich, J. F. Cochran, M. Kowalewski, J. Kirschner, Z. Celinski, A. S. Arrott and K. Myrtle, *Phys. Rev. B* **44**, 9348 (1991).
- ⁴⁵ R. W. Schoenlein, W. Z. Lin, J. G. Fujimoto and G. L. Eesley, *Phys. Rev. Lett.* **58**, 1680 (1987).
- ⁴⁶ P. B. Allen, *Phys. Rev. Lett.* **59**, 1460 (1987).
- ⁴⁷ U. Bovensiepen, *J. Phys.: Condens. Mat.* **19**, 083201 (2007).
- ⁴⁸ J. W. Kim, K. D. Lee, J. W. Jeong and S. C. Shin, *Appl. Phys. Lett.* **94** 192506 (2009)
- ⁴⁹ M. Wietstruk, A. Melnikov, C. Stamm, T. Kachel, N. Pontius, M. Sultan, C. Cahl, M. Welnet, H. A. Dürr and U. Bovensiepen, submitted
- ⁵⁰ G. M. Müller, J. Walowski, M. Djordjevic, G. X. Miao, A. Gupta, A. V. Ramos, K. Gehrke, Moshnyaga, K. Samwer, J. Schmalhorst, A. Thomas, A. Hütten, G. Reiss, J. S. Moodera and M. Münzenberg. *Nature Mat.* **8** 56 (2009).
- ⁵¹ X. A. Wang, S. H. Nie, J. J. Li, R. Clinite, J. E. Clarck and J. M. Cao, *Phys. Rev. B* **81** 220301 (2010).
- ⁵² J. Walowski, M. Djordjevic, M. D. Kauffman, B. Lenk, C. Hamann, J. McCord and M. Münzenberg, *J. Phys. D: Appl. Phys.* **41** (2008).
- ⁵³ S. Mizukami, H. Abe, D. Watanabe, M. Oogane, Y. Ando and T. Miyazaki, *Appl. Phys. Expr.* **1** 121301 (2008).
- ⁵⁴ B. D. Cullity, *Introduction to magnetic materials*, Addison-Wesley Publishing Co, 1972.
- ⁵⁵ E. Carpane, E. Mancini, C. Daller, M. Brenna, E. Puppini and S. De Silvestri, *Phys. Rev. B* **78** 174422 (2008).
- ⁵⁶ U. Atxitia, O. Chubykalo-Fesenko, R. W. Chantrell, U. Nowak and A. Rebei, *Phys. Rev. Lett.* **102** 057203 (2009).